

See discussions, stats, and author profiles for this publication at: <https://www.researchgate.net/publication/267705258>

# VARIABILITY IN THE FLORIDA CURRENT: IMPLICATIONS FOR POWER GENERATION

Article

---

CITATIONS

0

---

READS

77

3 authors, including:



[Alana Duerr](#)

U.S. Department of Energy

11 PUBLICATIONS 109 CITATIONS

[SEE PROFILE](#)



[J. H. VanZwieten Jr](#)

Florida Atlantic University

61 PUBLICATIONS 540 CITATIONS

[SEE PROFILE](#)

# VARIABILITY IN THE FLORIDA CURRENT: IMPLICATIONS FOR POWER GENERATION

Howard P. Hanson, Alana E. Smentek-Duerr, James H. VanZwieten, Jr.  
*hphanson@fau.edu*                      *asmentek@fau.edu*                      *jvanzwi@fau.edu*

*Southeast National Marine Renewable Energy Center  
Florida Atlantic University, 777 Glades Road, Boca Raton, Florida, USA*

## ABSTRACT:

THE FLORIDA CURRENT—the reach of the Gulf Stream System in the Straits of Florida—offers the potential for renewable base-load power for the energy-hungry southeast Florida metropolitan area, the seventh largest in the U.S. Realization of this potential requires, among other things, a better understanding of both the structure and variations of the flow in order to provide developers of marine hydrokinetic energy conversion devices with information critical to the design process and to quantify more completely the resource itself.

To this end, the Southeast National Marine Renewable Energy Center has deployed Acoustic Doppler Current Profilers (ADCPs) at a variety of locations offshore Fort Lauderdale. Resulting current profiles are discussed in this paper, with particular emphasis on observed variability and its implications for power generation.

## 1. INTRODUCTION

Compared to 2009, by 2035 total world electricity generation is projected to increase by nearly 84%, to the equivalent of some 4 TW ( $=10^{12}$  W) of continuous production (8). While much of this increase is projected to occur in the developing world, in order to satisfy U.S. demand for electricity, which is on track to increase by about 30%, it will be necessary to generate the continuous equivalent of about 585 GW ( $=10^9$  W) (7). Given the increasingly problematic reliance on fossil fuels to meet even existing demand, it seems clear that new sources of

energy for the future will be needed to accommodate these future consumption rates. It is only reasonable to suggest that these new energy sources should be diversified, clean, reliable, and cost effective (9). Such a diversified portfolio of energy sources for the future will undoubtedly include those both familiar and new. This paper is concerned with one of the newer energy sources, marine renewable energy (MRE).

In the open ocean, there exist two primary modes of MRE. *Hydrokinetic energy* in current systems such as the Gulf Stream, which can have the power density of gale force winds and more, can be converted to electricity using marine current turbine (MCT) technologies. *Thermal energy* in the oceanic stratification, which can be tapped using ocean thermal energy conversion (OTEC) technology (1;17), exists throughout the tropics and subtropics.<sup>1</sup> The Southeast National Marine Energy Center is working toward technology advancement and market acceleration for both of these MRE modes.

This paper is concerned with one aspect of technology advancement to harness hydrokinetic energy from the Florida Current. Clearly, designing MCT technology requires understanding the environment in which the devices are to be deployed. To move toward a better such understanding, we present here results from several sets of measurements of the Florida Current.

---

<sup>1</sup> The other modes of MRE, wave energy, tidal current & gravitational-potential energy, and the potential energy in salinity gradients are confined largely to coastal locations.

## 2. BACKGROUND

### 2.1 Data

SNMREC has deployed upward-looking Acoustic Doppler Current Profilers offshore Fort Lauderdale at two locations, the red dots in Fig. 1. In addition to the locations of the two profiler buoys, Fig. 1a, which is presented for purposes of illustration, shows bathymetry from the NOAA/NOS database and current speeds (colors) and directions (arrows) from the 1/25° HYCOM-NCODA assimilation (5;6) results from the operational integrations at the Naval Research Laboratory<sup>2</sup>. Figure 1b shows an east-west cross section along 26°N latitude, where the two buoys were located; this structure is consistent with observations (12;3). The total power in the cross-section estimated from (12)—that is, the power density as defined below integrated over the cross-section—is of the order 20 GW (10).

The offshore buoy, B2, was located relatively near the escarpment (the gray cluster of isobaths) marking the eastern edge of the Miami Terrace, on the western edge of the main core of the Florida Current (on this day, in the model), which flows just slightly to the east of due north. We discuss first observations from a 75-kHz ADCP deployed there from March 2009-March 2010, for which a 10-minute ON / 20-minute OFF duty cycle was employed, producing a 30-minute sampling interval.

Although the fastest current occurs near the surface, deployment of energy conversion systems there would interfere with the busy commercial shipping lanes. At 50 m, below the draft of ships in the Straits, the average current speed in this record is  $1.49 \text{ m s}^{-1}$ , which implies a power density of  $1,695 \text{ W m}^{-2}$ , the equivalent of a  $14 \text{ m s}^{-1}$  wind. The variability, however, is large—the standard deviation is  $0.3 \text{ m s}^{-1}$ , and, of more importance, the maximum speed is nearly three of these standard deviations above the mean at  $2.35 \text{ m s}^{-1}$ , which, in terms of power, is equivalent to tropical-storm strength winds, with power density a factor of four higher than the mean. At the same time, the histogram of current speeds in the ADCP dataset is skewed toward the high end, meaning that the minimum current ( $0.3 \text{ m s}^{-1}$ ) occurs very seldom—which implies the potential for relatively high capacity factors for appropriately designed systems.

At buoy B3, ADCPs were deployed for the month of March 2009 and from September-November, 2011. During the

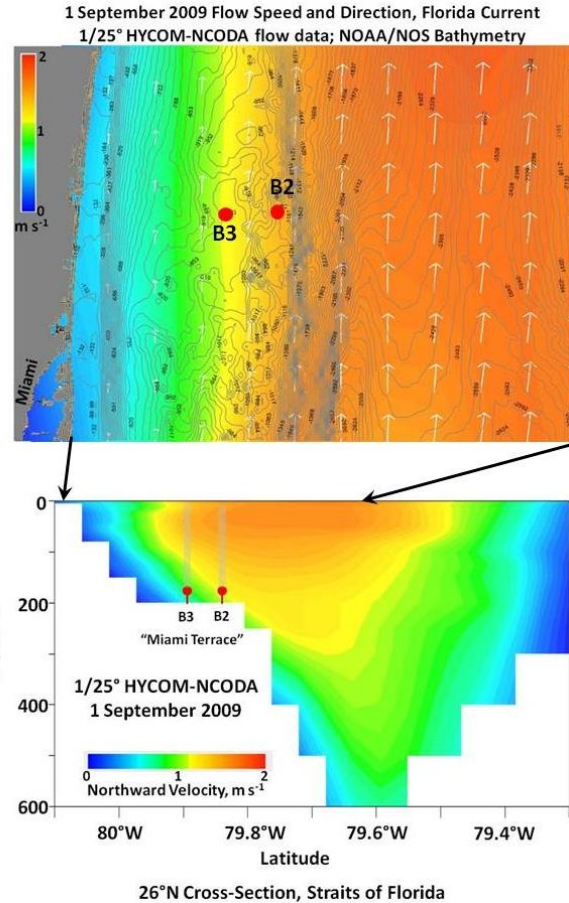


**Fig. 1: (a, top) Bathymetric chart offshore SE Florida with HYCOM-NCODA surface currents for 9/1/2009 superimposed. Buoy positions indicated by red dots. (b, bottom) E-W cross section across 26°N showing current structure and buoy positions.**

second of these deployments, the sampling interval was shortened from 30 minutes to 1 minute, and the higher time resolution provides an interesting look at higher frequency variations in somewhat lower-speed flows.

### 2.2 Power

Power generation by a moving fluid is proportional to the cube of the fluid velocity. For conventional axial-flow turbine systems, such as the now-familiar wind systems, it is convenient to define a *power density* [ $\text{W m}^{-2}$ ] as  $\Phi \equiv \frac{1}{2} \rho V^3$ , where  $\rho$  is the fluid density [ $\text{kg m}^{-3}$ ] and  $V$  is its velocity [ $\text{m s}^{-1}$ ], and an *effective (rotor) area* [ $\text{m}^2$ ] as  $A_E = \frac{1}{4} \pi D_T^2 C_P$ , where  $D_T$  [ $\text{m}$ ] is the diameter of the turbine's rotor and  $C_P$  is the system's power coefficient, an efficiency that is always less than about 0.6 (4).

<sup>2</sup> Data are publicly available from the server at HYCOM.org.

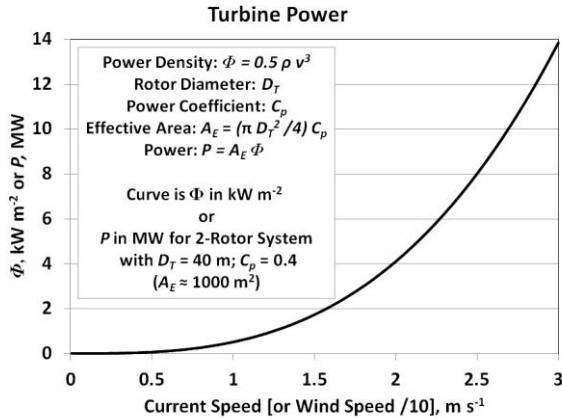


Fig. 2: Graph of cubic dependence of power on flow speed.

With these definitions, it is possible to write the power that a system can generate as the product of the turbine system parameters and the fluid properties:  $P = A_E \Phi$ .

It is useful to note that the ratio of the densities of water and air  $\rho_w / \rho_a \sim 1000$ , so that similar power densities are achieved in water that is moving about a tenth the speed of the wind. This is due to the cubic dependence of the power density on flow speed. However, from simple drag law considerations, this ratio of flow speeds results in forces in the water a factor of 10 greater than in the atmosphere, because the forces on structures in the two fluids scale as the *square* of the flow (10).

Purely for illustrative purposes, this paper hypothesizes a (rather ambitious) dual-rotor MCT system with a power coefficient  $C_p = 0.4$  and (two) 40-m rotors. This overall power coefficient is the product of the hydrodynamic

efficiency and the electromechanical efficiency of the MCT. Using the value of  $C_p = 0.4$  is reasonable, because peak rotor hydrodynamic efficiencies of 0.46 were found both experimentally for a tidal turbine by (2) and numerically for an ocean current turbine rotor (16), and electromechanical efficiencies for wind generators are typically around 90% (14), which yields an overall system efficiency of 0.41. These MCT parameters results in an effective area  $A_E = 1000 \text{ m}^2$ , so that it converts kilowatts per meter squared of power density into megawatts of power output (Fig. 2). Results discussed here can be transformed for more realistic MCT systems by scaling them by the appropriate  $A_E$ .

An important consideration for turbine system design and performance is the system's *cut-in speed*, the flow speed at which the rotor will begin to turn against its load and friction. As will be seen, cut-in speed is a significant factor in overall potential performance in the variable currents of the Straits of Florida.

### 3. ANNUAL VARIATIONS

A full understanding of annual variations, even at a single location, would require a decade or more of continuous measurements, so the year available from the Bouy 2 ADCP can provide only an example. Still, that example reveals several important results that have connection to MCT design and deployment.

Twelve months of the Bouy 2 dataset are depicted in Fig. 3, and it is apparent that variability occurs on a wide spectrum of time scales. The oceanographic processes responsible for this variability have been the subject of both observational and theoretical research for decades, and much of what is

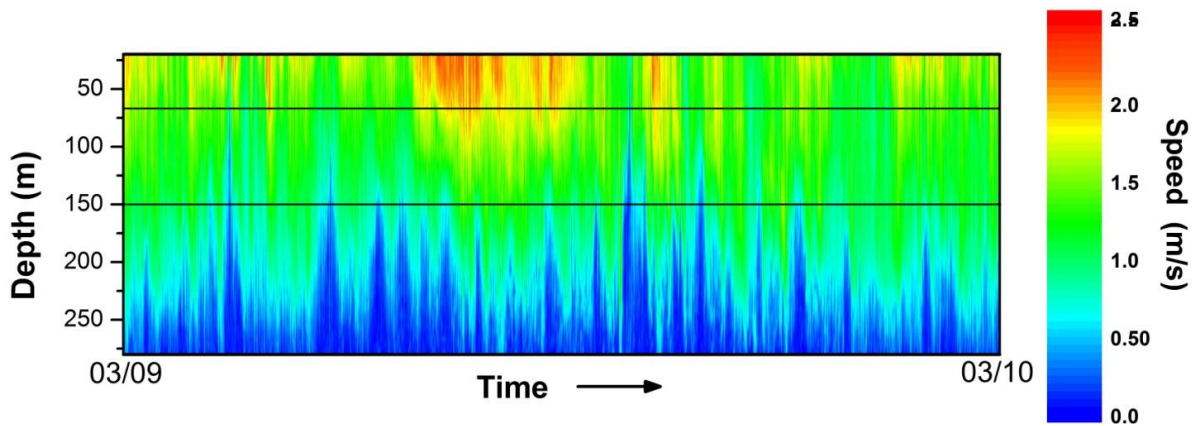


Fig. 3: Depth-time plot of current speed (colors) at Buoy 2, 12 month period beginning 1 March 2009. Horizontal lines are depth range considered in Fig. 6.

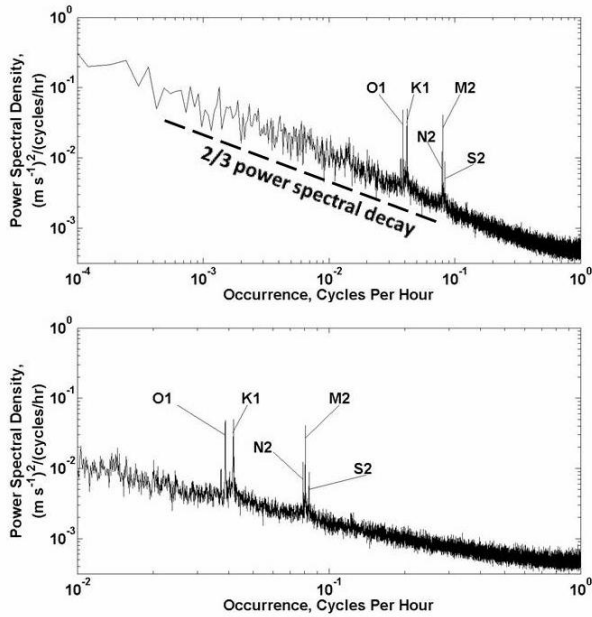


Fig. 4: Depth-averaged FFT power spectra of Buoy 2 data, with tidal frequencies annotated.

known about them today is the result of the Subtropical Atlantic Climate Studies (STACS) sponsored by the U.S. National Oceanic and Atmospheric Administration (15).

A first look at variations in this dataset is shown in the power spectra of Figs. 4. The top panel shows a wide-band spectrum encompassing time scales from about one day to about 100 days with a consistent  $\frac{2}{3}$  red-noise decay throughout and some indications of a leveling off at the high-frequency end (note that one cycle per hour is the Nyquist frequency here). Of note—and emphasized in the expanded high-frequency part of the spectrum in the bottom panel—are the tidal frequencies. In the figures to follow, the K1 (diurnal) tide is particularly apparent.

One question that might be asked concerns the performance of the hypothetical  $A_E = 1000 \text{ m}^2$  MCT system if it had been deployed at the position of Buoy 2 during this time period. Given the variation of current speed with depth that is apparent in Fig. 3, it is clear that this performance will depend on deployment depth.

Figure 5 shows the annual total energy to be expected from the hypothetical MCT, in  $\text{MW}\cdot\text{hr yr}^{-1}$ , if deployed at 70 m (blade tips at 50 m, just below surface shipping) and several deeper levels, all as a function of the MCT cut-in speed. The effect of the overall decrease of the current speed with depth

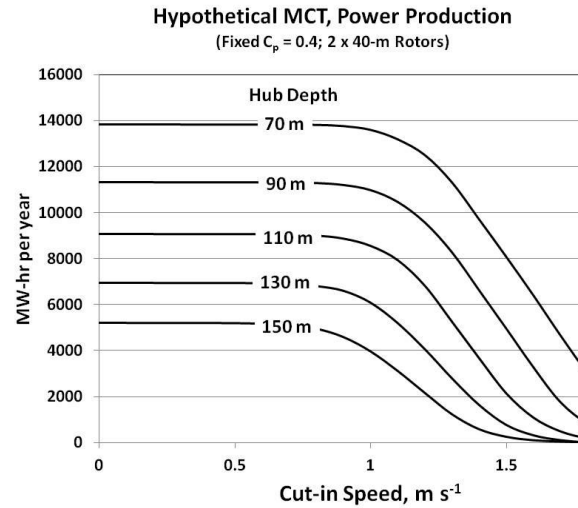


Fig. 5: Annual power production by the hypothetical  $A_E = 1000 \text{ m}^2$  MCT system when deployed at various depths, shown as a function of system cut-in speed.

is clear from the various ordinate crossings, each of which represents the maximum possible energy generation at that depth. The subsequent plateau as cut-in speed increases is due to two effects: the cubic dependence of  $\Phi$  on flow speed means that the initial increase is small in any case, and, for the most part, the minimum flow speed at these depths does not fall much below the value of the cut-in speed on the graph.

This all changes at a cut-in speed of approximately  $1 \text{ m s}^{-1}$ , where the plateau breaks into consistent fall-off of annual energy generation. Simply put, at higher and higher cut-in speeds, the MCT operates less of the time because the flow is slower than what is required to turn the MCT rotor. This is illustrated clearly in Fig. 6, where the white areas depict the times when the MCT is inoperable for 1, 1.25, and  $1.5 \text{ m s}^{-1}$  cut-in speeds, respectively.

The main lesson from this exercise concerns the effort that should be expended into optimizing cut-in speed, a problem involving both blade and rotor design as well as component design with respect to system friction. Clearly, it makes little sense, in this circumstance, to invest in R&D necessary to get cut-in speed much below  $1 \text{ m s}^{-1}$  (i.e., 2 kt).

#### 4. SPATIAL VARIATIONS

During part of the first month of the Buoy 2 deployment (March, 2009), a second 75-kHz ADCP was deployed at Buoy 3, about 8 km inshore from Buoy 2. Although in general (and certainly in Fig. 1) the flow at Buoy 3 is slower than at Buoy 2, during this time period they were rather similar. The time-depth plots for the two coincident datasets are shown in Fig. 7.

Commercial-scale deployments of MCTs will undoubtedly involve multiple systems, much as wind turbines are installed in “wind farms.” As can be inferred from Fig. 2, it would take 500 of the hypothetical MCTs discussed here to generate 1,000 MW in a  $1.5 \text{ m s}^{-1}$  (3 kt) flow. Even using a 3-dimensional array design, with MCTs at more than a single depth and with up/downstream E-W rows, a 500-system array would likely occupy several kilometers cross-stream. Spatial variations in power production on such scales are therefore of interest.

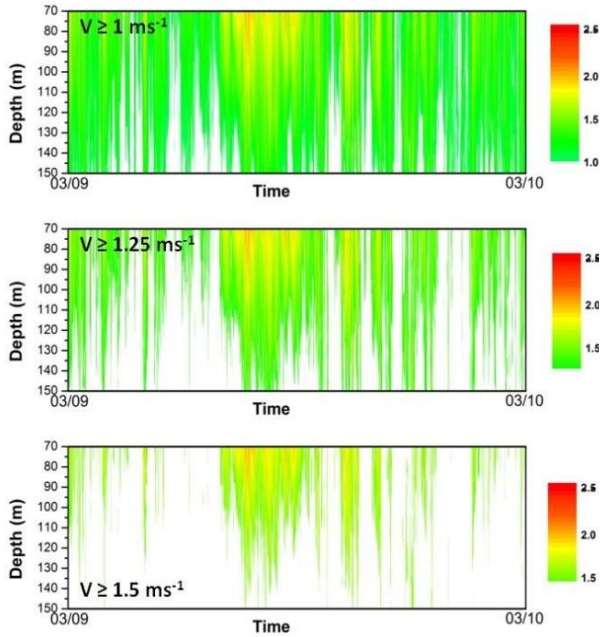


Fig. 6: Operational down-time (white) for the period March 2009—March 2010 for the hypothetical MCT at three cut-in speeds.

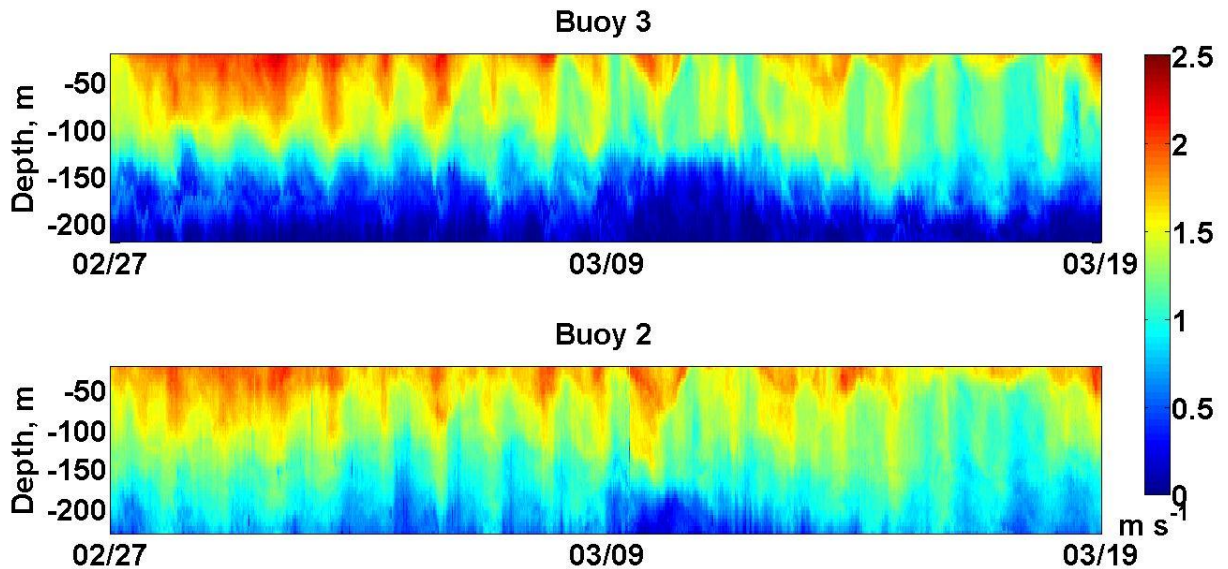
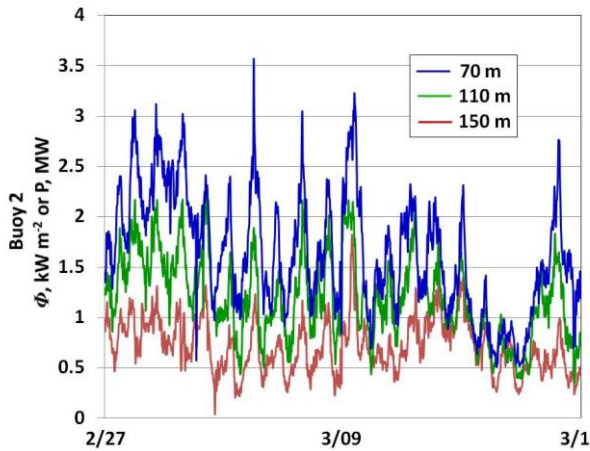
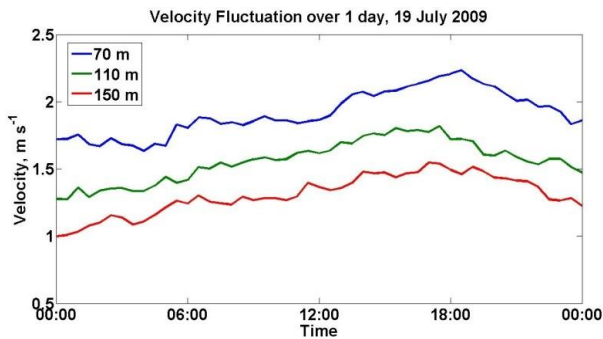


Fig. 7: Time-depth plots of current speeds for two 75-MHz ADCPs at Buoy 2 & 3 for the first part of March, 2009.



**Fig. 8: Power density  $\phi$ , for the hypothetical MCT systems discussed here, power at three depths at Buoy 2, for the time period of Fig. 7.**

The dominant variations in Fig. 7 are obviously caused by the diurnal tide, and visual inspection of the two records suggests that the variations are close to being in phase. A lag correlation analysis verifies this with the exception of a slight lag of Buoy 2 at 70 m. Higher resolution time samples are required to analyze this in detail. However, it is an important consideration, because significant lags imply that power production across an array on these spatial scales will not have synchronous variability. This has clear implications for the design of the power handling and conditions systems for the array. For example, Fig. 8 shows Buoy 2 power densities (and power amounts, for the hypothetical  $A_E = 1000 \text{ m}^2$  MCT systems) for the time period of Fig. 7 at three depths. At 70 m, the values range over a factor of 7, and some of the changes are quite abrupt, occurring on time scales of order an hour. Power handling in



**Fig. 9: Buoy 2 velocities at three depths, 19 July 2009.**

an out-of-phase array with systems subject to such changes could be challenging.

## 5. SHORT TIME SCALES

Although the variations on the diurnal time scale are obviously dominated by tidal signals, as can be seen from Fig. 7, additional variability is superimposed as well. For example, Fig. 9 shows one day of Buoy 2 data at the three depths shown in Fig. 8.

Although small, the sample-to-sample variations in velocity are of order 5% of the average signal and much larger than the measurement uncertainty (which is about  $0.04 \text{ m s}^{-1}$ ), which, given the cubic dependence, translates into a 15% variation in power densities. Again, issues for power management, particularly in arrays, arise.

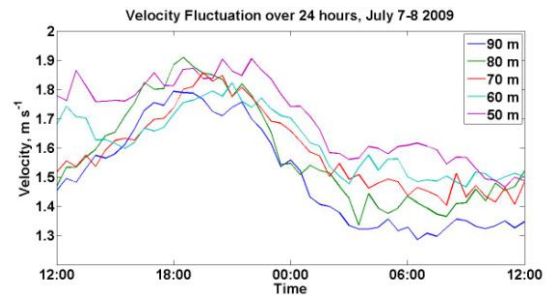


**Fig. 10: Current speeds over the span of a 40-m rotor. Braiding of the records implies reversals of out-of-plane torque on an MCT rotor would result. Note expanded vertical axis compared to Fig. 9.**

Of potentially more interest are velocity fluctuations across the scale of an MCT rotor. Figure 10 depicts current speeds over a 24-hour period during July, 2009. Although the diurnal tidal signal dominates the variability on that time scale, on shorter time scales there are times at which the vertical shear actually reverses. Generally, the current speed decreases with depth, which implies an out-of-plane torque on the MCT tending to pitch its nose up, but shear reversals would cause that torque to push the nose down. Pitch control is clearly an issue in this circumstance, and potential shaft-bearing issues are also of concern.

A final example of short-term variability is of interest, one that involves not so much fluctuations in current speed, and therefore forces on the equipment, but rather the current's direction. Although it may be expected that single MCTs would follow current directional changes, if moored properly, the behavior of multiple systems in an array is

another matter altogether. Because it is likely that systems will be deployed within tens of rotor diameters of each other, for economic reasons and to try to capture as much of the current's energy as possible, large current directional changes, especially those with on scales smaller than the array itself, have the potential to cause havoc.

And such a potential exists. During a second deployment of an ADCP at Buoy 3 in the Fall of 2011, the local current underwent two reversals. These are depicted using current vectors in Fig. 11.

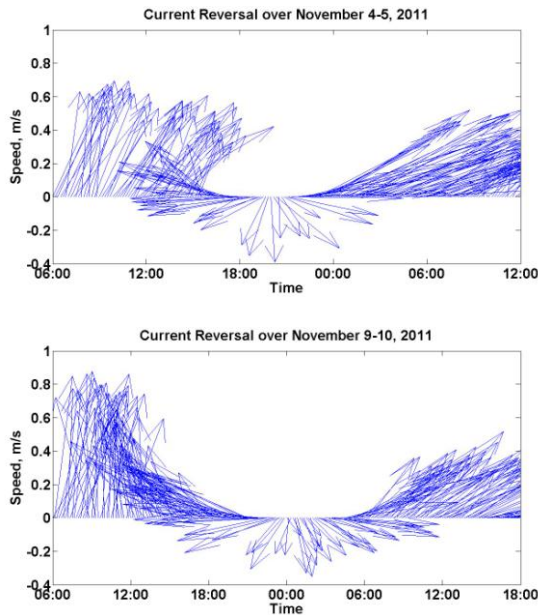


**Fig. 11: Current vector time series showing brief current reversals during November, 2011.**

Among the various physical processes causing variability in the Florida Current, it has been known for some time that cyclonic spin-off eddies, often originating far to the south of the instruments at the SNMREC buoys, propagate northward along the Florida coast and cause southward flow near shore (13). The implication here is that deployments need to be far enough offshore to avoid such eddies.

## 6. CONCLUSION

The challenges associated with development of MRE resources are significant. Many of them involve environmental interactions—the effects of MCT deployments on oceanic ecosystems, for example, are completely unknown and may or may not be an issue with respect to federal and state environmental laws and

regulations. Because environmental interactions work both ways, though, it is also important to understand the effects of the marine environment on the MRE equipment to be deployed. In addition to materials-related issues (corrosion and biofouling are likely to be huge hurdles), there is the overall issue of MCT design and its optimization for particular locations.

Developing the MRE resources of open-ocean current systems such as the Florida Current will require detailed site characterization studies for locations of interest. This paper discusses aspects of one such study for the Florida Current offshore Fort Lauderdale and the use of traditional oceanographic measurements in non-traditional ways to infer strategies to meet some of the development challenges. It is worth noting that model results can also be used in such non-traditional ways (11).

One example of such non-traditional use of oceanographic data is shown in Fig. 5. The annual record of current speed from an ADCP deployment at SNMREC Buoy 2 is used there to infer potential annual energy production as a function of MCT system cut-in speed. These results clearly show the value of optimize blade design so as to decrease cut-in speed up to a point—efforts to decrease cut-in speed below about  $1 \text{ m s}^{-1}$  are shown there to have marginal value. While this result is specific to the particular location of these measurements, it is like that other such conclusions can be drawn based on observations taken at potential deployment sites.

Although analysis of these datasets provides insight into variability on scales longer than a few minutes, at the current speeds in the records this implies spatial scales of variability—eddies—on scales 100-200 m. Variability on scales smaller than this, that is, turbulence down to the dissipation scale, is likely to be important for turbine design as well. Thus, turbulence measurement as part of site characterization becomes an important priority for future work.

## 7. ACKNOWLEDGMENTS

The Southeast National Marine Renewable Energy Center is supported with funds from the State of Florida and from the U.S. Department of Energy. We thank the SNMREC program and operations staff—Bill Baxley and Shirley Ravenna deserve special mention—for their dedication to obtaining the datasets discussed here.



## 8. REFERENCES

- (1) Avery, W.H. and C. Wu: *Renewable Energy From The Ocean - A Guide To OTEC*. Oxford University Press, 480pp. ISBN-13: 978-0195071993, 1994
- (2) Bahaj, A. S., A.F. Molland, J.R. Chaplin, W.M.J. Batten : Power and thrust measurements of marine current turbines under hydrodynamic flow conditions in a cavitation tunnel and a towing tank, *Journal of Renewable Energy*, **32**:407-426, 2007
- (3) Beal, L.M., J.M. Hummon, E. Williams, O.B. Brown, W. Baringer, and E.J. Kearns: Five years of Florida Current structure and transport from the Royal Caribbean Cruise Ship *Explorer of the Seas*. *Journal of Geophysical Research*, **113**:C06001/1-11, 2008
- (4) Betz, A.: Introduction to the Theory of Flow Machines. (D. G. Randall, Trans.) Oxford: Pergamon Press, 1966
- (5) Chassignet, E.P., H.E. Hurlburt, O.M. Smedstad, G.R. Halliwell, P.J. Hogan, A.J. Wallcraft, R. Baraille, and R. Bleck: The HYCOM (HYbrid Coordinate Ocean Model) data assimilative system, *Journal of Marine Systems*, **65**:60-83, 2007
- (6) Chassignet, E.P., H.E. Hurlburt, E.J. Metzger, O.M. Smedstad, J.A. Cummings, G.R. Halliwell, R. Bleck, R. Baraille, A.J. Wallcraft, C. Lozano, H.L. Tolman, A. Srinivasan, S. Hankin, P. Cornillon, R. Weisberg, A. Barth, R. He, F. Werner, and J. Wilkin: US GODAE: Global ocean prediction with the HYbrid Coordinate Ocean Model (HYCOM). *Oceanography*, **22**:64-75, 2009
- (7) EIA (Energy Information Administration, U.S. Dept. of Energy): *Annual Energy Outlook 2011, with Projections to 2035*. Report DOE/EIA-0383(2011), U.S. Dept. of Energy, Washington, DC. Available at <http://www.eia.gov/forecasts/aeo/pdf/0383%282011%29.pdf>, 2011
- (8) EIA: *International Energy Outlook 2011*. Report DOE/EIA-0484(2011), U.S. Dept. of Energy, Washington, DC. Available at <http://205.254.135.24/forecasts/ieo/pdf/0484%282011%29.pdf>, 2011
- (9) Hanson, H.P.: Diversified renewables. *EnergyBiz*, **6**(4):52, 2009
- (10) Hanson, H. P., S.H. Skemp, G.M. Alsenas, and C.E. Coley, 2010: Power from the Florida Current: A new perspective on an old vision. *Bulletin of the American Meteorological Society*, **91**, 861-866, doi: 10.1175/2010BAMS3021.17.
- (11) Hanson, H.P., A. Bozec, and A.E.S. Duerr: The Florida Current: A clean but challenging energy resource. *Eos: Transactions of the American Geophysical Union*, **92**:29-30, 2011.
- (12) Leaman, K.D., R.L. Molinari, and P.S. Vertes: Structure and variability of the Florida Current at 27°N: April 1982—July 1984. *Journal of Physical Oceanography*, **17**:565-583, 1987
- (13) Lee, T.N.: Florida Current spin-off eddies. *Deep Sea Research and Oceanographic Abstracts*, **22**:753-765, 1975
- (14) Li, H., and Chen, Z.: Overview of different wind generator systems and their comparisons, *IET Renewable Power Generation*, **2**:123-138, 2008
- (15) Molinari, R.L.: Subtropical Atlantic Climate Studies (STACS): An update. *Oceanography*, **12**:32-35, 1989
- (16) VanZwieten, J. H., Jr., C.M. Oster, and A.E.S. Duerr: Design and analysis of a rotor blade optimized for extracting energy from the Florida Current. *Proceedings of the ASME 2011 International Conference on Ocean, Offshore, and Arctic Engineering*, Rotterdam, Netherlands, June 19-24, . OMAE2011-49140, 2011
- (17) Vega, L.A.: Ocean thermal energy conversion primer, *Marine Technology Society Journal*, **36**:25-41, 2003